RESEARCH AND DEVELOPMENT TECHNICAL REPORT
SLCET-TR-90-16

FABRICATION AND CHARACTERIZATION OF YTTRIUM BARIUM COPPER OXIDE SUPERCONDUCTORS FOR MICROWAVE APPLICATIONS

DOUGLAS J. BASARAB, MICHELLE A. DORNATH-MOHR,
DONALD W. ECKART, ROBERT D. FINNEGAN, JOSEPH P. KLIMEK,
ERNEST POTENZIANI II, WILLIAM D. WILBER
U.S. ARMY ELECTRONICS TECHNOLOGY AND DEVICES LABORATORY

AND

WILLIAM SAVIN, LEO M. SILBER, ART TAUBER (GEO-CENTERS, INC.)
CHRISTOPHER S. WRENN (VITRONICS, INC.)

JANUARY 1991

US ARMY
LABORATORY COMMAND
FORT MONMOUTH, NEW JERSEY 07703-5000

NOTICES

Disclaimers

The findings in this report are not to be construed as an official Department of the Army position, unless so designated by other authorized documents.

The citation of trade names and names of manufacturers in this report is not to be construed as official Government indorsement or approval of commercial products or services referenced herein.

REPORT DOCUMENTATION PAGE

Form Approved
OMB No. 0704-0188

1. AGENCY USE ONLY (Leave blank)	2. REPORT DATE	3. REPORT TYPE AND DATES COVERED
	January 1991	Technical Report: 1987 to 1989

4. TITLE AND SUBTITLE
FABRICATION AND CHARACTERIZATION OF YTTRIUM BARIUM COPPER OXIDE SUPERCONDUCTORS FOR MICROWAVE APPLICATIONS

5. FUNDING NUMBERS
PE) 1L161102
PJ) AH47
TA) EE
WU) DA313762

6. AUTHOR(S)
Douglas J. Basarab, Michelle A. Dornath-Mohr, Donald W. Eckart, Robert D. Finnegan, Joseph P. Klimek, Ernest Potenziani II, William D. Wilber, (contd, Block 11)

7. PERFORMING ORGANIZATION NAME(S) AND ADDRESS(ES)
US Army Laboratory Command (LABCOM)
Electronics Technology and Devices Laboratory (ETDL)
ATTN: SLCET-EA
Fort Monmouth, NJ 07703-5000

8. PERFORMING ORGANIZATION REPORT NUMBER
SLCET-TR-90-16

9. SPONSORING/MONITORING AGENCY NAME(S) AND ADDRESS(ES)

10. SPONSORING/MONITORING AGENCY REPORT NUMBER

11. SUPPLEMENTARY NOTES
(6. AUTHORS, contd:) William Savin (Geo-Centers, Inc.), Leo M. Silber (Geo-Centers), Art Tauber (Geo-Centers), Anup Tilak (Geo-Centers), Christopher S. Wrenn (Vitronics, Inc.)

12a. DISTRIBUTION/AVAILABILITY STATEMENT
Approved for public release; distribution is unlimited.

12b. DISTRIBUTION CODE

13. ABSTRACT (Maximum 200 words)

High temperature superconductors offer several advantages over normal conductors for low power device applications. Bulk ceramic processing parameters are investigated to define optimum conditions for materials useful in microwave applications. Calcining, sintering, and reaction atmosphere were systematically varied in bulk samples. The density, microstructure and composition, dc resistivity, microwave Q, and surface resistivity were followed as a function of sintering temperature. An optimum sintering temperature is defined.

14. SUBJECT TERMS
Superconductors, Ceramics, Microwaves, Processing

15. NUMBER OF PAGES
29

16. PRICE CODE

17. SECURITY CLASSIFICATION OF REPORT	18. SECURITY CLASSIFICATION OF THIS PAGE	19. SECURITY CLASSIFICATION OF ABSTRACT	20. LIMITATION OF ABSTRACT
Unclassified	Unclassified	Unclassified	UL

CONTENTS

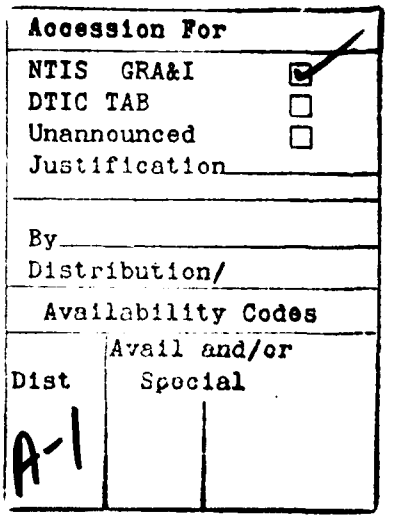

FIGURES

TABLES

INTRODUCTION

Since the discovery of high T_c superconductors in 1986 there have been many investigations of the relationships between bulk fabrication parameters and physical properties. There is however, very little known about the relationship between microwave properties, other physical properties and fabrication parameters. The purpose of the research described in this report was to identify fabrication parameters which would sensitively affect microwave properties of $YBa_2Cu_3O_{7-x}$, (hence forth referred to as 123).

High T_c superconductors are of great interest to the Army and DOD; applications appear feasible in the early 1990's time frame. Low power microwave device applications offer advantages over devices fabricated from normal conductors. If the surface resistance of the superconductor is less than that of a normal conductor, such as copper, at the operating frequency, one expects insertion losses to be reduced, signal to noise ratios enhanced, while dissipation of heat is negligible. In addition, there are unique properties possessed by superconductors which may be exploited for device applications.

EXPERIMENTAL

A major goal of this investigation is the development of a synthesis process for the fabrication of various bulk geometrics. Since the literature [1-4] describes processing methods based primarily on Y_2O_3, $BaCO_3$ and CuO as the precursors for 123 and these are commercially available with reasonable purities, phase diagrams with these as components were sought. The lower temperature range of interest was set by results of earlier studies which indicated that one needs to sinter 123 above 900°C to achieve bodies with useful properties. The most appropriate phase diagrams are shown in Figs. 1a and b. In Fig. 1a one notes the pseudo binary join between 123, labeled 1/6 $YBa_2Cu_3O_{7-x}$ and CuO, labeled line A. The phase diagram representing this join is shown in Fig 1b. The formation of a liquid phase at 900°C continues above 1000°C. Therefore the experimental plan employs the sintering range of 900 to 1000°C.

---

1. W.J. Nellis and L.D. Woolt, MRS Bulletin 63, 1989.
2. D.W. Murphy, D.W. Johnson, Jr., S. Jinb, R.E. Howard, Science 241 922 (1988).
3. XlaO-Dong Chen, Sang Younglee, John P. Golben, Sung-IK, R.D. McMichael, Yi Song Tae, W. Noh, and J.F. Gaines, Rev Sci Instrum 58 1565 (1987).
4. K.C. Goretta, M.T. Lanagan, J.P. Single, J.T. Dusek, V. Balachandran, S.E. Dorrin, and R.B. Poeppel, Material and Manufacturing Processes 4 (2) 163 (1989).
5. Kunihiko Oka, Kenji NaKane, Masahiko Ito, Masatoski Saito, and Hiromi Unoki, Jap J Appl Physics 27, L1065 (1988).

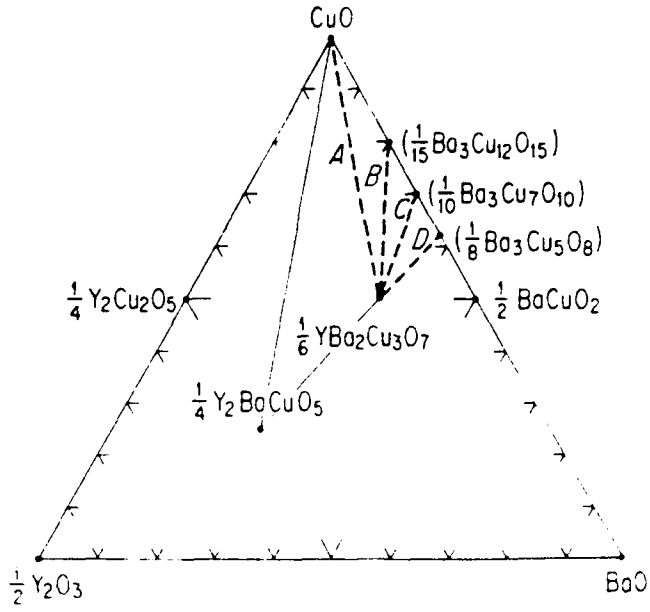

Figure 1a. The Y_2O_3-BaO-CuO ternary phase diagram.

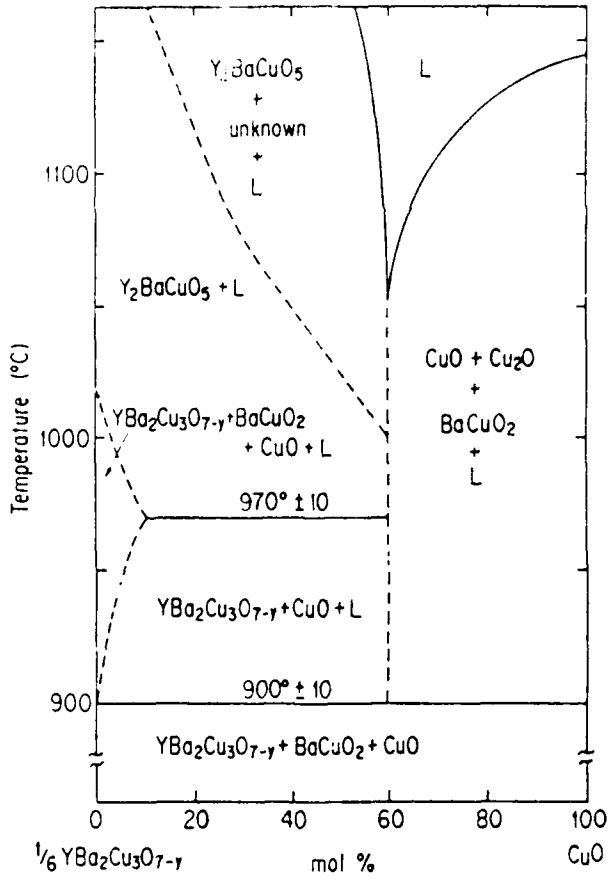

Figure 1b. The pseudo binary phase diagram in the ternary Y_2O_3-BaO-CuO system.

Material Preparation

In this investigation, all 123 samples were prepared from CP grade CuO, Y_2O_3 and $BaCO_3$. The powders were pre-dried, weighed out and dry mixed in an attritor mill or "Wigly Bug" several times. They were subsequently pressed into discs 1/8-1/4 inch in thickness, 3/4-1 inch in diameter and calcined in air, vacuum or an inert atmosphere. The product was reground in a mill to about 100 microns particle size, repressed and fired at least twice (Appendix A). After the final calcination the powder was jet milled to an average particle size of 2-3 microns. The powder was then pressed at 20,000 psi in a steel die and formed into a disc or cylinder, depending upon the final application. Pressed pieces were placed in a polyethylene bag and the latter sealed. This was then sealed in a second bag. The double bag configuration was placed in an isostatic press and subjected to a pressure of 50 to 55 kpsi. Isostatically pressed pieces were placed on setter plates coated with 123 powder and fired according to the oxygen sintering schedule (Appendix A). In every instance pieces were fired in flowing oxygen at a pressure slightly greater than 1 atmosphere.

Material Characterization

After jet milling, the 123 powders were examined by CuK x-ray diffractometry. Most powders had broad diffraction peaks of reduced intensity due to the small particle size and strain developed as a consequence of milling. If secondary phases were present, their diffraction peaks were in the noise of the diffraction traces. The jet milled powder had a mean particle size ranging from 2-3 microns with many smaller particles and a few particles as large as 10 microns. Figure 2 shows two typical examples.

Sintered samples exhibited much sharper diffraction patterns than calcined material, and contained weak diffraction peaks due to such compounds as CuO, $BaCuO_2$, Y_2BaCuO_5. These secondary phases could be observed in the metallurgical microscope and SEM in polished specimens Figs. 3b and 4. The light colored nontabular grains are CuO which crystallized on solidification from a partial melt during sintering and filled the space between the tabular 123 phase. The composition of the CuO phase was confirmed with EDAX in the SEM.

RESULTS

Microstructure

The 123 grains observed in polished sections in a metallurigical microscope with Nomarski optics are typically tabular and grow in size with increasing sintering temperature,

from 900-980°C (Fig. 3). Grains as large as 400 microns have been observed. Review of x-ray diffraction line intensity indicates that these grains are randomly aligned. For large grains, greater than 10 microns, twinning is observed (Fig. 5). For samples with sintering temperatures at and above 960°C, holes arising from liquid phase formation are observed (Figs. 3 C,D). For samples sintered above 950°C, cracks sometime appear parallel to the long direction of grains (Fig. 6). Cracking arises in large grains and propagates, due to stress arising from a polymorphic phase transition, upon cooling.

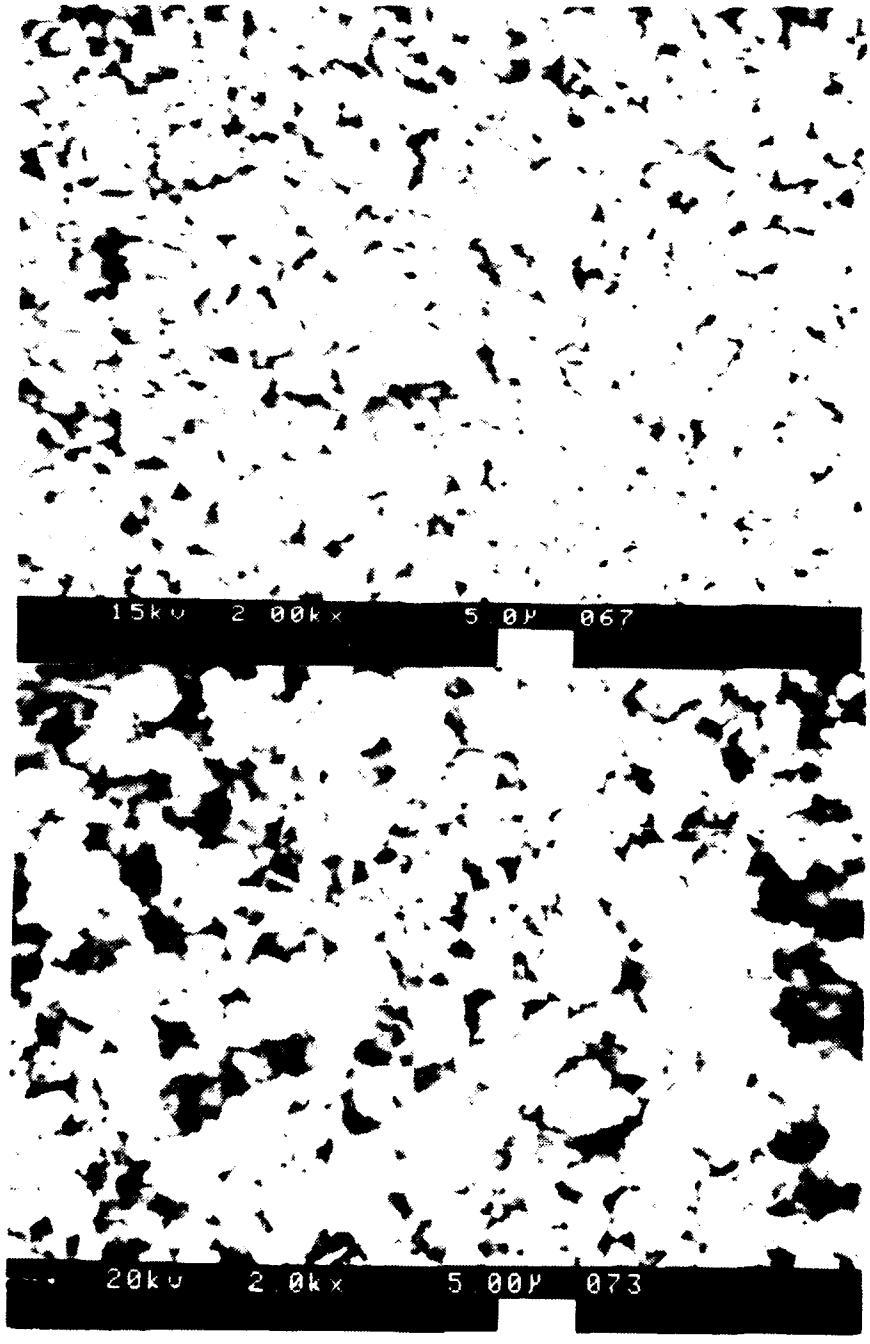

Figure 2. Two SEM micrographs showing particle size and morphology of calcined, jet milled 123 powder before pressing and sintering.

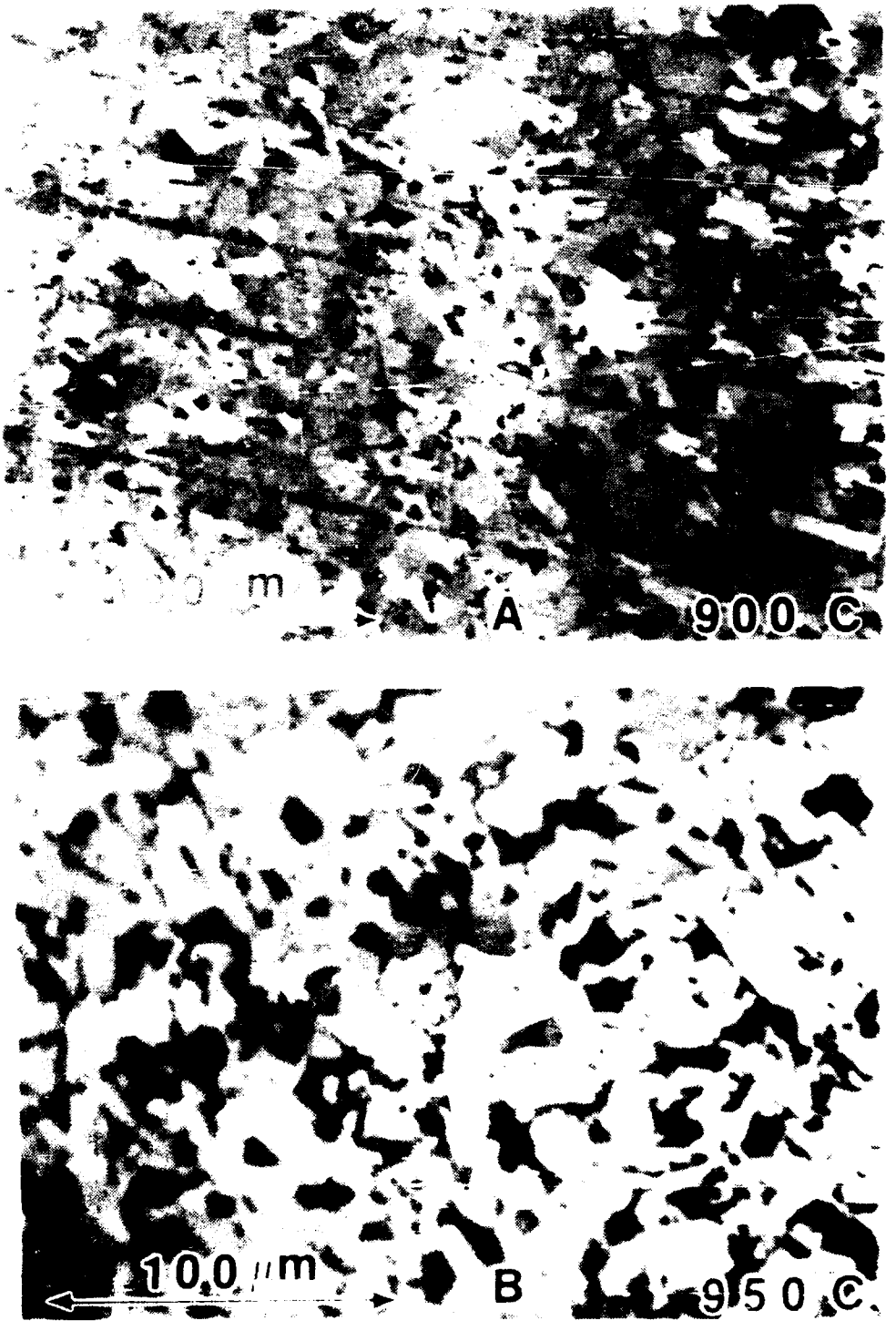

Figure 3. Micrographs of polished sections using a metallurgical microscope with Nomarski optics for samples sintered at a) 900°C, b) 950°C, c) 960°C, and d) 980°C.

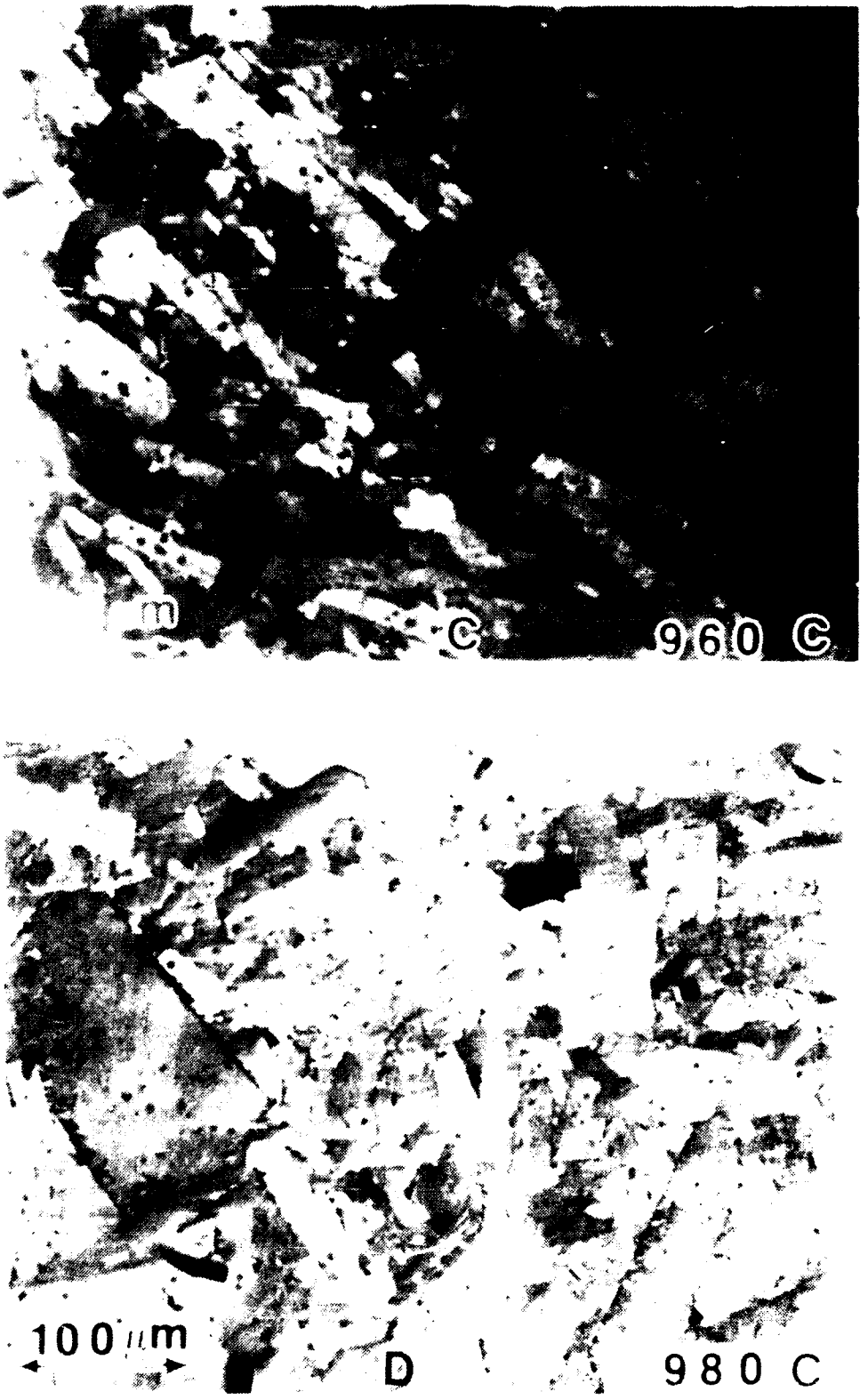

Figure 3. Micrographs of polished sections using a metallurgical microscope with Nomarski optics for samples sintered at a) 900°C, b) 950°C, c) 960°C, and d) 980°C (continued).

Figure 4. Scanning electron micrograph of polished cross-section of sample sintered at 950°C.

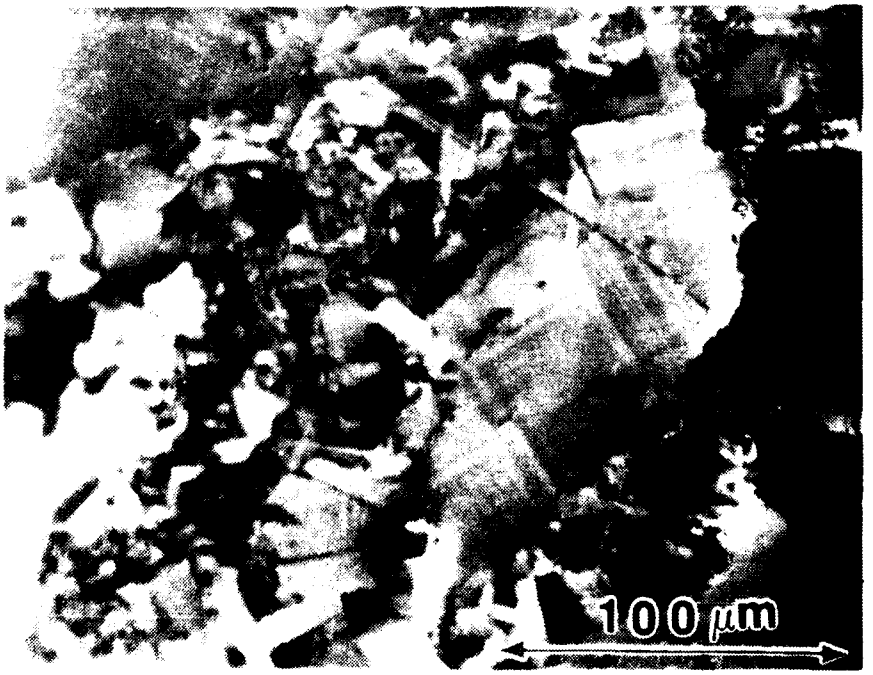

Figure 5. Micrograph of polished section using a metallurgical microscope with Nomarski optics showing twinning of large grains.

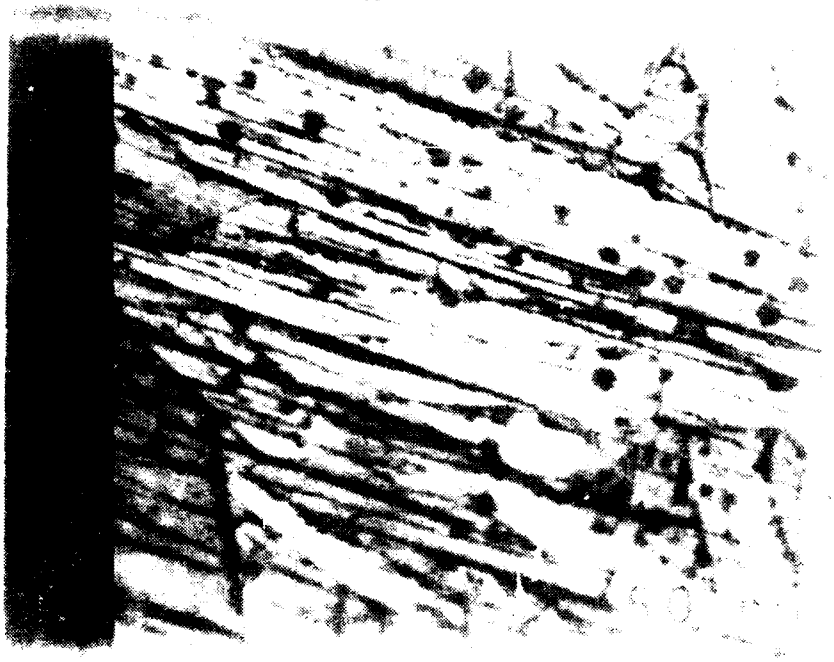

Figure 6. Micrograph of polished section using a metallurgical microscope with Nomarski optics showing cracking.

Density

Density measurements were carried out on cubes cut from sample discs. Volumes were determined from dimensional data obtained with a micrometer and mass was determined with an analytical balance. The percent of theoretical density versus sintering temperature is plotted in Fig. 7. With increasing sintering temperature the density increases, reaches a maximum at about 950°C, and declines with increasing temperature. The observed trend may arise from the competition of two processes. $YBa_2Cu_3O_{7-x}$ begins to melt incongruently at about 900°C. Three phases are present: $YBa_2Cu_3O_{7-x}$, CuO and a liquid. The liquid serves as a sintering aid helping to increase the density. With increasing temperature this phenomenon increases. At the same time that sintering and densification are enhanced, secondary phases are also forming. These phases may be less dense and may also increase the porosity. A maximum in density is achieved near 950°C. Above this temperature, degradation due to secondary phases outweighs the benefits of liquid sintering and density decreases.

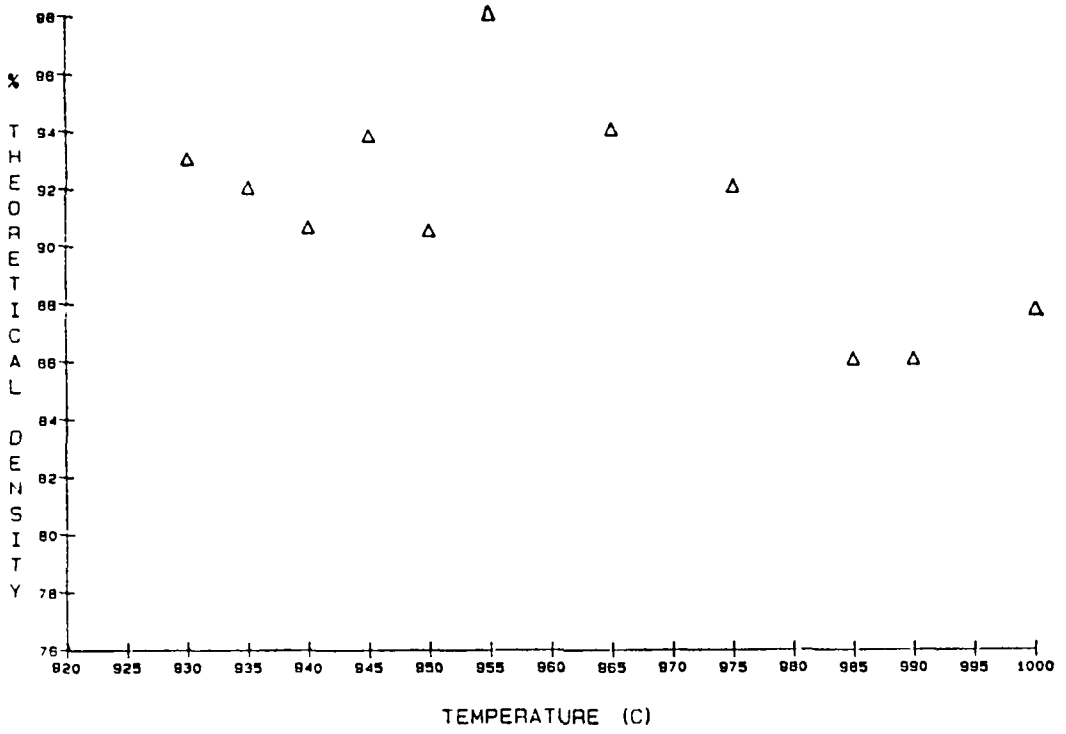

Figure 7. Percent theoretical density versus sintering temperature.

DC Resistance

The dc resistance was measured as a function of temperature from 300 to 10 K using the four probe technique. The automated measuring system employed a closed cycle refrigerator. All samples exhibited metallic behavior down to the superconducting transition (Appendix B.) The variation in the width of the transition as a function of temperature was similar to the density behavior (Table 1). The width of the transition decreased as the sintering temperature was raised above 900°C, reached a minimum at 950°C, then increased for temperatures higher than 950°C.

Microwave Properties

The property of greatest interest is the surface resistance because many microwave applications depend upon materials with as small a magnitude in this parameter as possible. The variation of surface resistance as a function of frequency and temperature was investigated. The method used employed a resonant cavity and the surface resistivity was determined from the change in the unloaded Q of the cavity upon insertion of a sample.

TABLE 1. R/R_O VERSUS T

SINTERING TEMP °C	T_C	TRANSITION REGION K	WIDTH K
910	89.4	87.7 - 91.2	3.5
920	90.7	89.7 - 91.6	2.0
930	89.9	89 - 90.8	1.8
940	90.9	89.9 - 91.9	2.0
950	90.2	89.7 - 90.8	1.1
960	90	89.0 - 91.0	2.0
965	91	89.9 - 91.9	2.0

One spectrometer operated in the 8.1-9.5 GHz (X band) range. Its cavity had a Q of about 56,000 at 77 K. A flow diagram for the spectrometer is shown in Fig. 8. Measurements were made at liquid nitrogen temperature by putting a plastic bag around the cavity and its stainless steel waveguide feed and dipping the cavity into a plastic foam dewar filled with liquid nitrogen. A waveguide window was inserted in the waveguide feed and dry helium gas blown into the cavity to prevent condensation of moisture in the cavity. A thermocouple on the outside of the cavity monitored its temperature. This sample arrangement made it possible to measure a large number of samples 2 K above liquid nitrogen temperature.

Discs were prepared by grinding samples as fired to 0.75 inch diameter and about 0.1 inch thick. A series of discs sintered at different temperatures were glued on the end plate of the TE_{011} cavity with Duco cement and the Q was measured. For a sample of these dimensions, one can calculate the ratio of surface resistivity of the sample (Rs) to that of silver (R_{Ag}) as a function of the ratio of the Q of the empty cavity, Q_1, to that of the cavity with sample, Q_2.

The calculated surface resistivity for this series of samples ranged from a high of 177 to a low of 27 times the surface resistivity of silver at 79 K. It is unfortunate that those measurements could not be made at lower temperatures because subsequent measurements on other samples showed that the surface resistivity changes rapidly in this temperature region. In several samples, the surface resistance dropped by 35% in lowering the temperature from 79 K to 75 K.

X-Band Microwave System for Measurement of Q

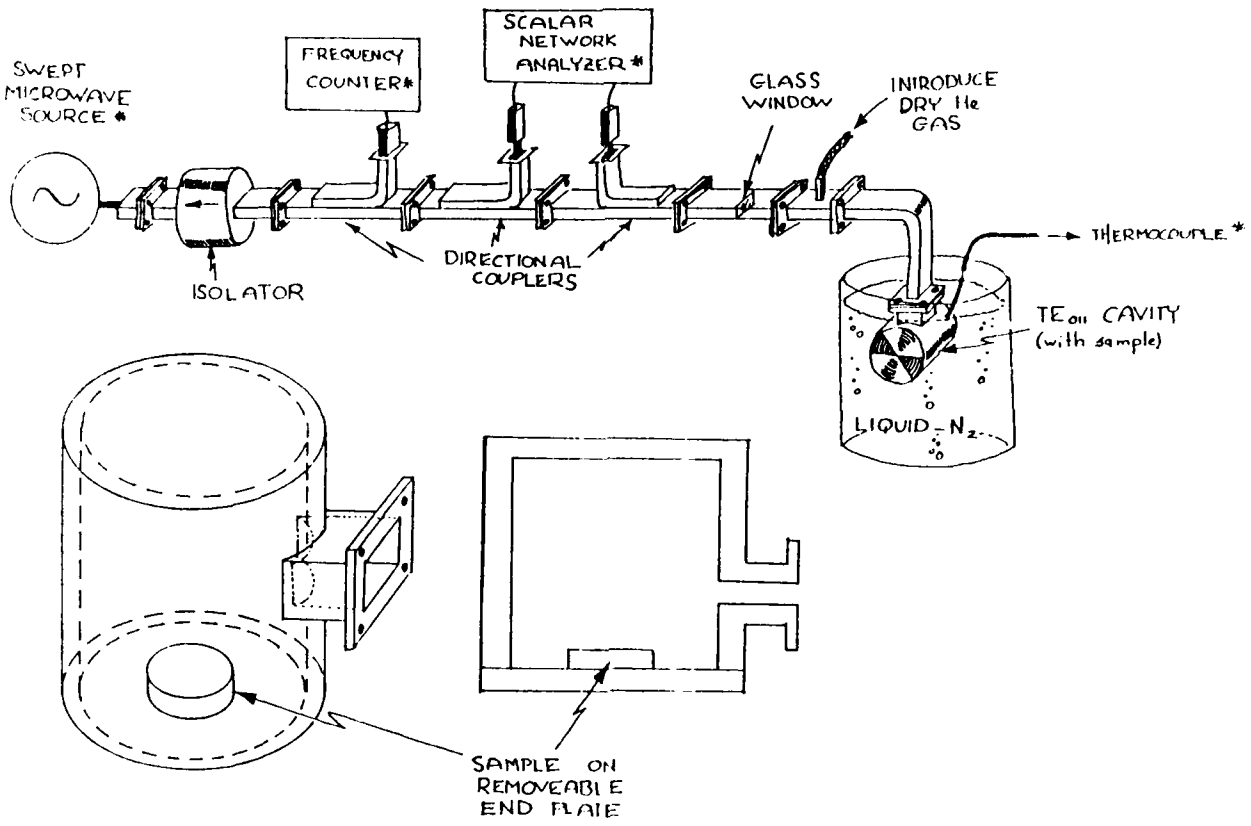

Figure 8. Flow diagram for the X-Band Microwave System for measurement of Q.

The surface resistance as a function of temperature behaved in a similar manner as the density and dc resistance, i.e., with the best results obtained on samples sintered at a temperature close to 950°C.

Better results were obtained on samples vacuum calcined and sintered for 72 hours. The results are:

$$R_s(\text{sample})/R_{Ag} = 1.26 \text{ to } 2.74$$

A second spectrometer was designed for 26.5 to 40 GHz (Ka-band) operation and was used with a high-Q, copper cavity resonant at 35 GHz. The 35 GHz cavity is different from the X-band cavity in that the sample is used as one complete end-plate of the cylindrical cavity, not attached to the end-plate. For the 35 GHz cavity, the volume of the cavity remains constant while one end-plate consists of either a copper disc (used as a standard) or a superconducting disc. Furthermore, the 35 GHz cavity is fastened to a liquid-helium cooled cryostat so that the R_s can be measured at any temperature from 10 to 300 K.

The considerable size difference between the X-band and Ka-band cavities (the volume of the 35 GHz cavity is less than 10% that of the X-band cavity volume) is the reason why the Ka-band cavity can be cooled with a liquid-helium cryostat while the X-band cavity is cooled in a liquid nitrogen bath. The smaller cavity also affords the use of the sample as an end-plate; the X-band cavity would require a sample diameter greater than 1.5 inches for a geometry similar to the 35 GHz cavity.

Prior to the measurement of the 3/4 inch diameter discs, the samples were first polished and then heated in oxygen. The samples were polished with #600 (if necessary), #800, #1000, #1200, #2400 and #4000 Struers silicon carbide paper. The discs were then heated in oxygen according to the schedule in Table 2. The samples were stored in a dry oxygen atmosphere upon removal from the furnace.

The two parameters that are measured in the microwave experiment are the cavity Q and resonance frequency. As an example of the measured data, Fig. 9 shows the Q and resonance frequency for the 35 GHz cavity with the 965°C (sintering temperature) sample in place. From these data, one can calculate R_s as a function of temperature for the superconducting sample.

The surface resistivity for three samples, annealed at temperatures of 950, 965, and 975°C, was obtained in the manner just described and the results, along with the experimentally determined R_s values for copper, are shown in Fig. 10. There are several features of Fig. 10 that should be noted. First, the general trend for R_s of each superconducting sample is to decrease with temperature, starting near the critical temperature of about 93 K. Typically, the normal-state resistivity is sufficient to degrade the Q to a value that can no longer be measured. However, the 950°C sample exhibited a normal-state R_s that could still be determined at temperatures above T_c. Note that the data sets labeled 975 and 975 (B) represent measurements of opposite sides of one disc. The difference in R_s for these two data sets illustrates the unavoidable variation in electrical properties even within the same batch of material.

TABLE 2. Furnace program for polished discs

Step #	Operation	Time
0	start at 200°C	2 hrs
1	warm to 450°C	10 hrs
2	cool to 400°C	2 hrs

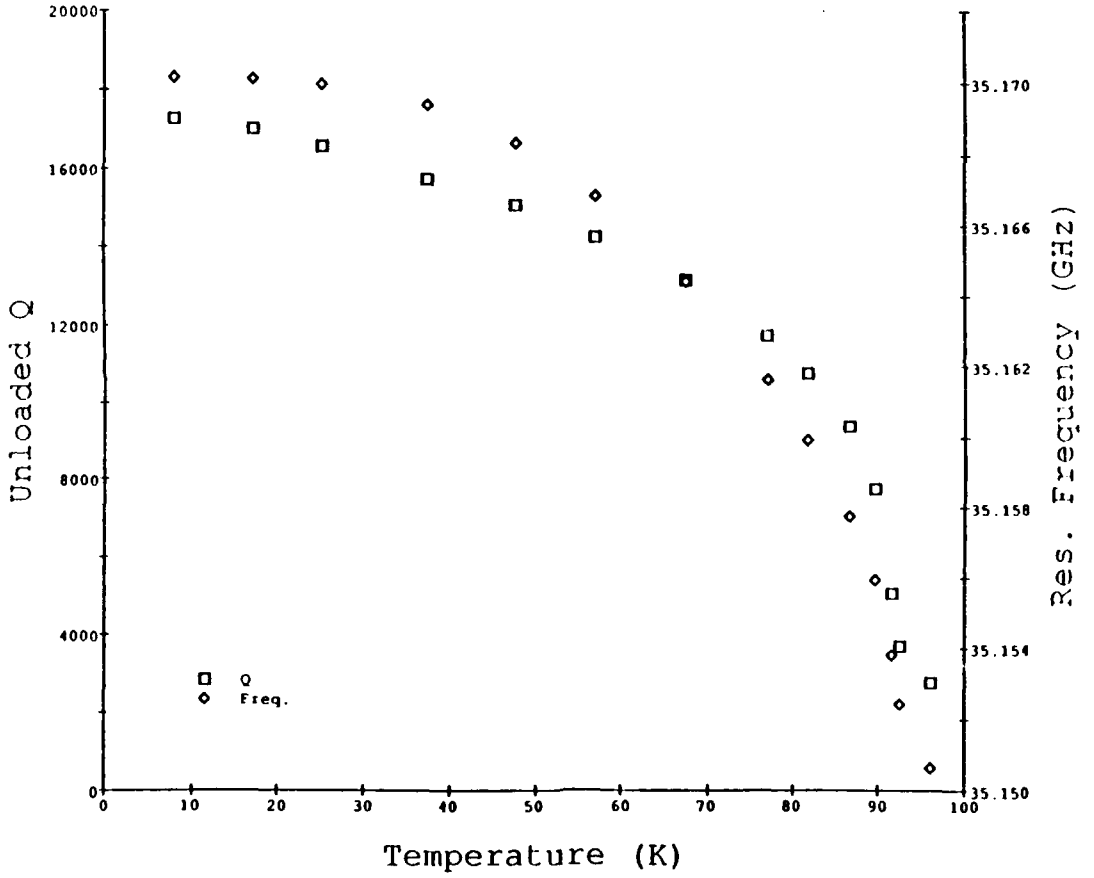

Figure 9. Measured Q and resonance frequency for the 35 GHz cavity with a superconducting disc, annealed at 965°C, at one end of the cavity (the sample position).

The second important feature of Fig. 10 is that none of the samples exhibit an R_S value below that of copper at the same temperature. This comparison with copper is the ultimate test of a superconductor's usefulness at a particular frequency. The 950°C sample shows the lowest R_S, yet is still inferior to copper; at 20 K, R_S=0.05 ohm for the 950°C sample and R_S=0.03 ohm for the copper standard. It should be noted here that the R_S values in Fig. 10 were obtained roughly one year after the samples were fabricated, and that the samples are known to degrade somewhat with time. Earlier measurements at 32 GHz, made shortly after the samples were fabricated, employed a cavity coupling scheme that was less reproducible (therefore less accurate) than the current system. These earlier measurements, however, indicated that R_S for the 965°C sample was nearly equal to R_S for copper at 10 K; the margin of error was estimated to be 0.010 ohm.

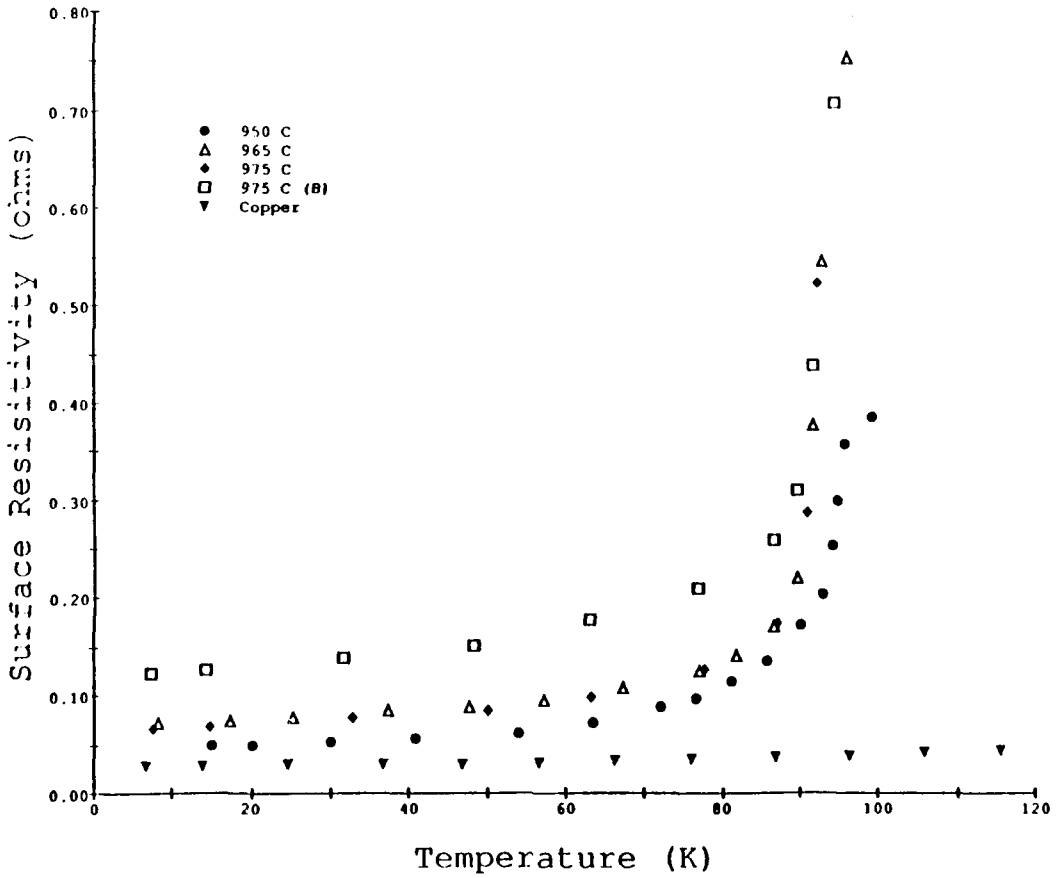

Figure 10. Surface resistivity as a function of temperature for three superconducting samples annealed at 950, 965, and 975°C. The data sets labeled 975 and 975 (B) are for opposite sides of the same disc. The data set for an OFHC copper disc is included for comparison.

Since the surface resistivity of a superconductor varies as the square of the frequency [6,7], one can use the results of Fig. 10 to estimate R_s at various frequencies for each of the three samples. Furthermore, since R_s for a normal conductor varies as the square root of the frequency, one can define a "crossover frequency" at which, for a chosen temperature, R_s for the superconductor equals R_s for copper; below the crossover frequency, the surface resistivity of the superconductor is superior to that of copper, while above the crossover frequency, R_s for copper is less than R_s for the superconductor. Table 3 is a list of the crossover frequencies calculated for each sample at temperatures of 20 K and 77 K. For the best sample (950°C anneal), the 20 K crossover frequency is 24.9 GHz and the 77 K crossover is 16.7 GHz.

The 77 K crossover frequencies listed in Table 3 imply that the surface resistivity of the superconductors at 8 to 10 GHz should be superior to the R_s for copper. However, 8 GHz X-band measurements show that R_s for the superconductors is 1.26 to 2.74 times the value for silver. The higher R_s values may be due to the fact that for the X-band measurement, the entire sample is placed inside the cavity whereas only one side of the disc is measured at 35 GHz. Furthermore, only the samples measured at 35 GHz were polished and then heated in oxygen prior to the measurement.

TABLE 3. Crossover frequencies extrapolated from 35 GHz measurements

Sample	@ 20 K	@ 77 K
950°C	24.9 GHz	16.7 GHz
965°C	16.1 GHz	13.7 GHz
975°C	17.6 GHz	14.0 GHz
975°C	11.7 GHz	10.2 GHz

6. A. Fathy, D. Kalokitis and E. Belohoubek, Microwave Journal 31 (10), 75 (1988).
7. T. VanDuzer and C.W. Turner, Principles of Superconductive Devices and Circuits (Elsevier, New York, 1981).

Millimeter-wave measurements were not limited to disc-shaped samples. In an effort to make a superconducting cavity, cylinders of the 123 material were pressed, machined and polished (inner surface only) so that they could be used as a cylindrical TE_{011} cavity resonant at 35 GHz. The cylinders were approximately 0.62 inch long with an inside diameter of 0.468 inch and outside diameter of 0.750 inch. Copper end-plates were used and a coaxial feed was brought through the center of one end-plate. The cylinders were cooled using the liquid-helium flow cryostat mentioned previously. Figure 11 is a graph of the resonator Q as a function of temperature. For comparison, the Q of an all-copper cavity is included along with a horizontal line that indicates the room-temperature Q of the copper cavity. One can see that the Q obtained with the 123 cylinder is superior to the Q measured for room-temperature copper but is below the Q of the cooled copper cavity.

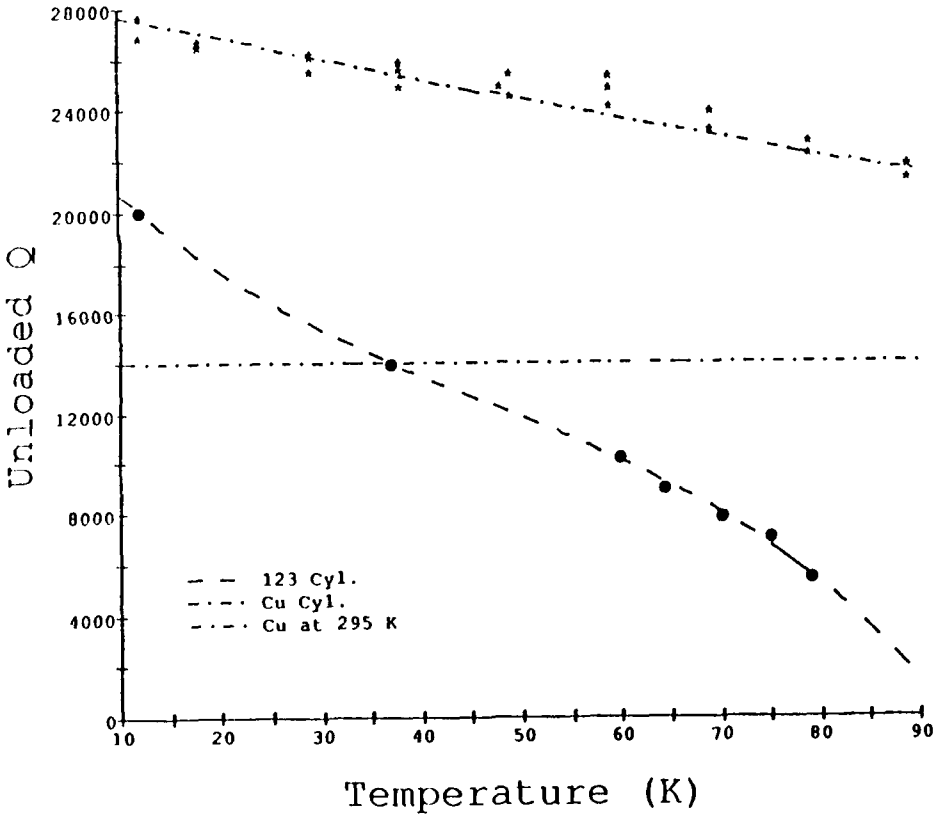

Figure 11. Q as a function of temperature for a cavity formed from a superconducting cylinder and for a copper cavity. The horizontal line indicates the room temperature Q for the copper cavity.

CONCLUSIONS

In order to fabricate useful military microwave devices one should start with materials that exhibit microwave surface resistivities that are at least an order of magnitude smaller than Cu at 77 K.

The microwave surface resistance obtained in this investigation on bulk discs and cavities at 8.1 GHz and 35 GHz between Tc and 10 K has rarely fallen below that of Cu at the corresponding temperature and frequency. The more important causes for this are materials-oriented problems. Major ones are the presence of secondary phases in the grain boundaries which act as weak links as well as discrete precipitates which reduce the number of percolation paths. Other problems include the lack of orientation, the presence of which would serve to reduce the resistivity; and the presence of point and line defects arising from elemental impurities, cracks, dislocations and strains which are manifest in twinning and polytypism.

Secondary phases can be eliminated by using more reactive precursors. One route is the use of coprecipitated precursors formed from homogeneous solutions. Pyrolysis of these materials leads to solid state reactions and formation of the 123 at lower temperatures and with finer particles than can be achieved by calcination and sintering. Because the latter requires elevated temperatures, large grain growth is encountered. One seeks to avoid this because large grains (in excess of 1 micron) help to propagate cracks. Chemical reactions leading to full crystallization and densification at lower temperatures also reduces dislocations and stress due to polymorphic phase transition. Enhanced orientation can be achieved in bulk material by appropriate application of a magnetic field at temperatures above Tc. This takes advantage of the anisotropy in the paramagnetic susceptibility. This can be exploited even further by replacing some or all of the yttrium in 123 with rare earths having a large number of unpaired electrons and large spin orbital coefficient or anisotropic g factors.

APPENDIX A

HEATING SCHEDULES

A. Calcining Program in Air

Segment	Function	Time (hrs)	Temperature (°C)
1	hold	0.5	300
2	ramp	6	300
3	soak	15	900
4	ramp	3	900
5	ramp	5	700
6	hold	10	400
7	ramp	1	400
8	ramp	1	300

B. Calcining in Vacuum

Segment	Function	Time (hrs)	Temperature (°C)
1	hold	0.5	25
2	ramp	4	600
3	hold	manual	600 until outgassing is completed
4	ramp	3	900
5	hold	12	900
6	ramp	6	25

C. Sintering in Oxygen

Segment	Function	Time (hrs)	Temperature (°C)
1	hold	1	300
2	ramp	6	300
3	hold	10-72	sintering
4	ramp	10	sintering
5	hold	20	650
6	ramp	5	650
7	hold	20	400
8	ramp	1	400
9	ramp	1	300

APPENDIX B

RESISTANCE CURVES

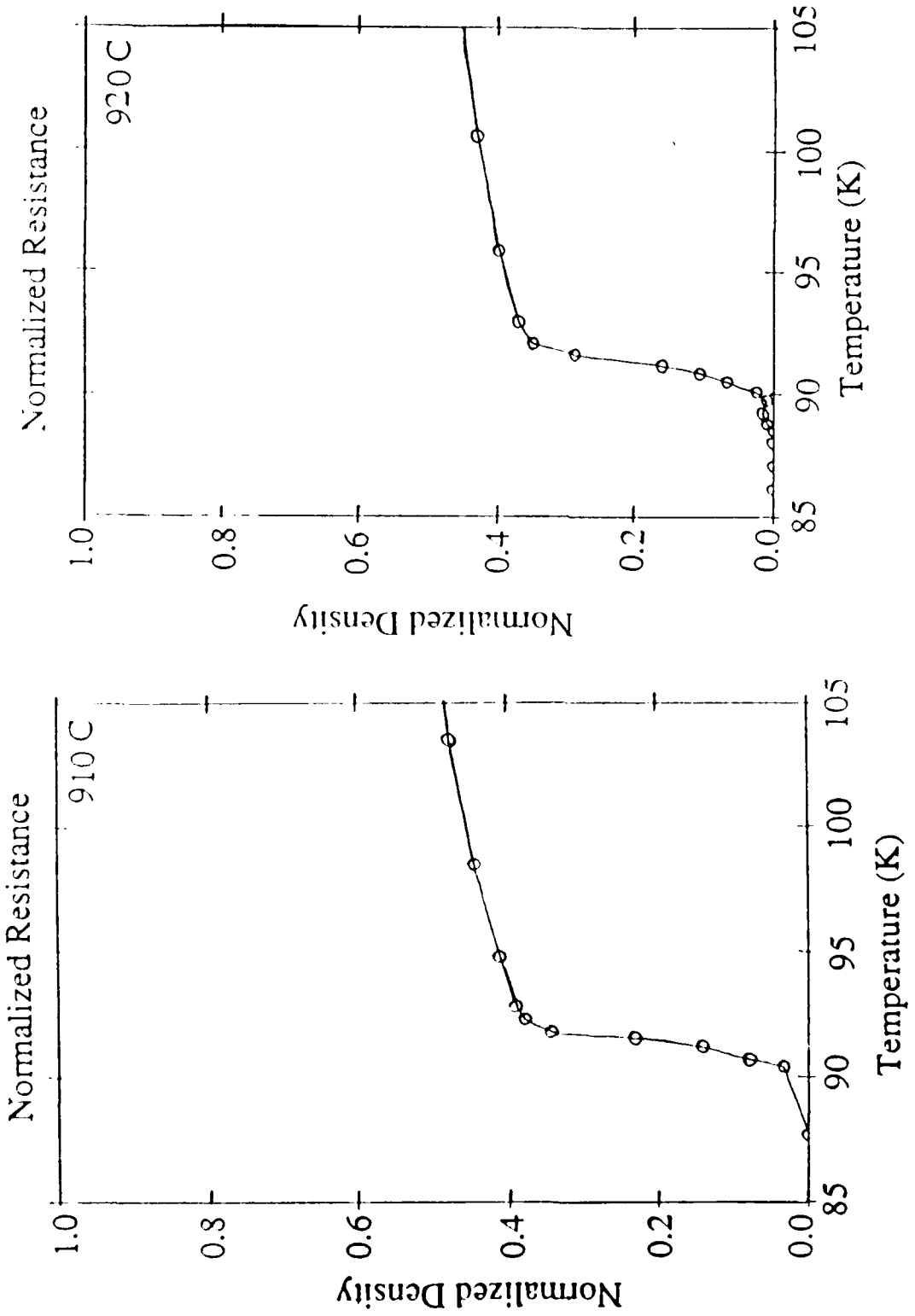

Figure 12. Normalized resistance for sample sintered at a) 910°C, b) 920°C c) 950°C, and d) 960°C.

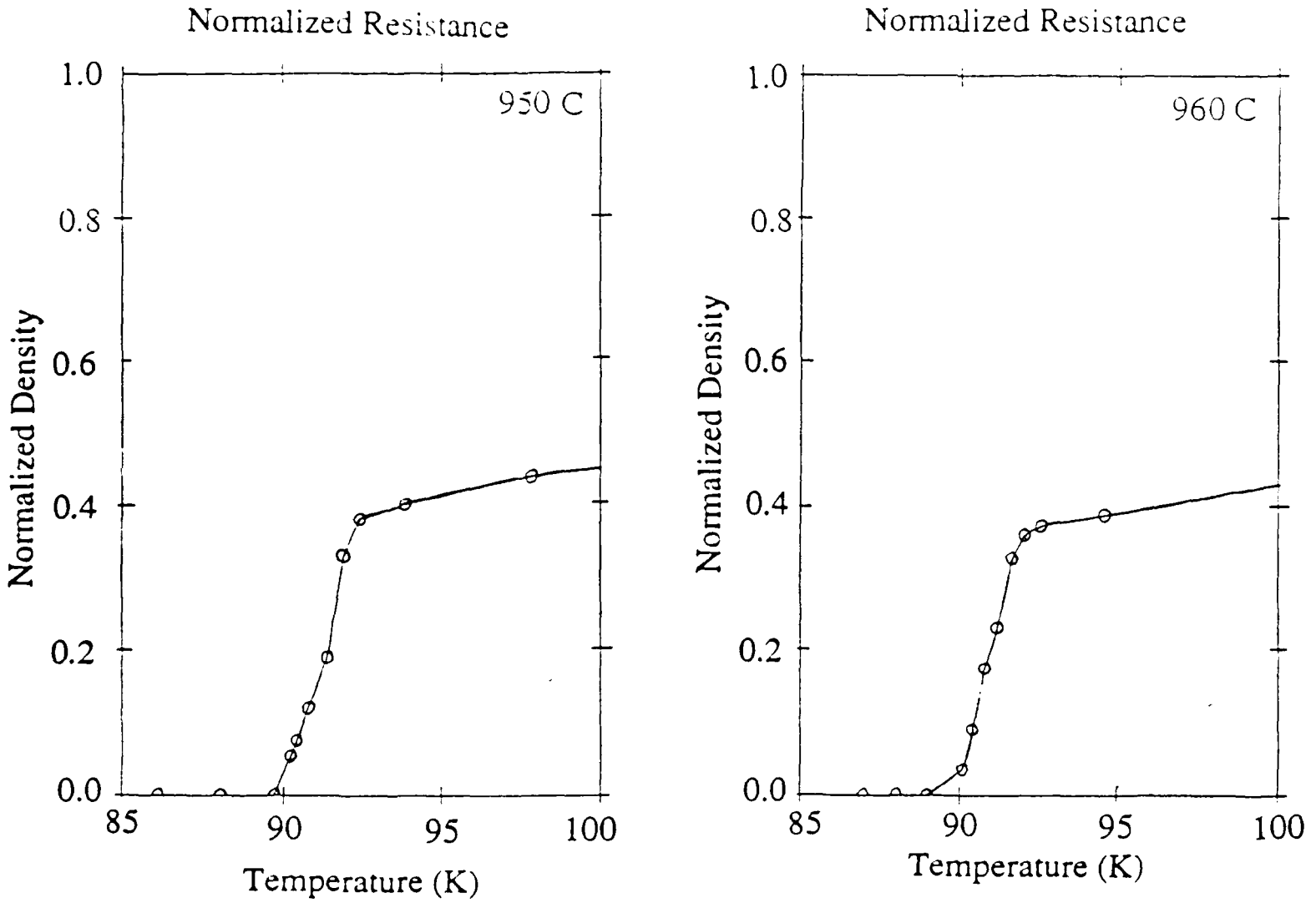

Figure 12. Normalized resistance for sample sintered at a) 910°C, b) 920°C, c) 950°C, and d) 960°C (continued).

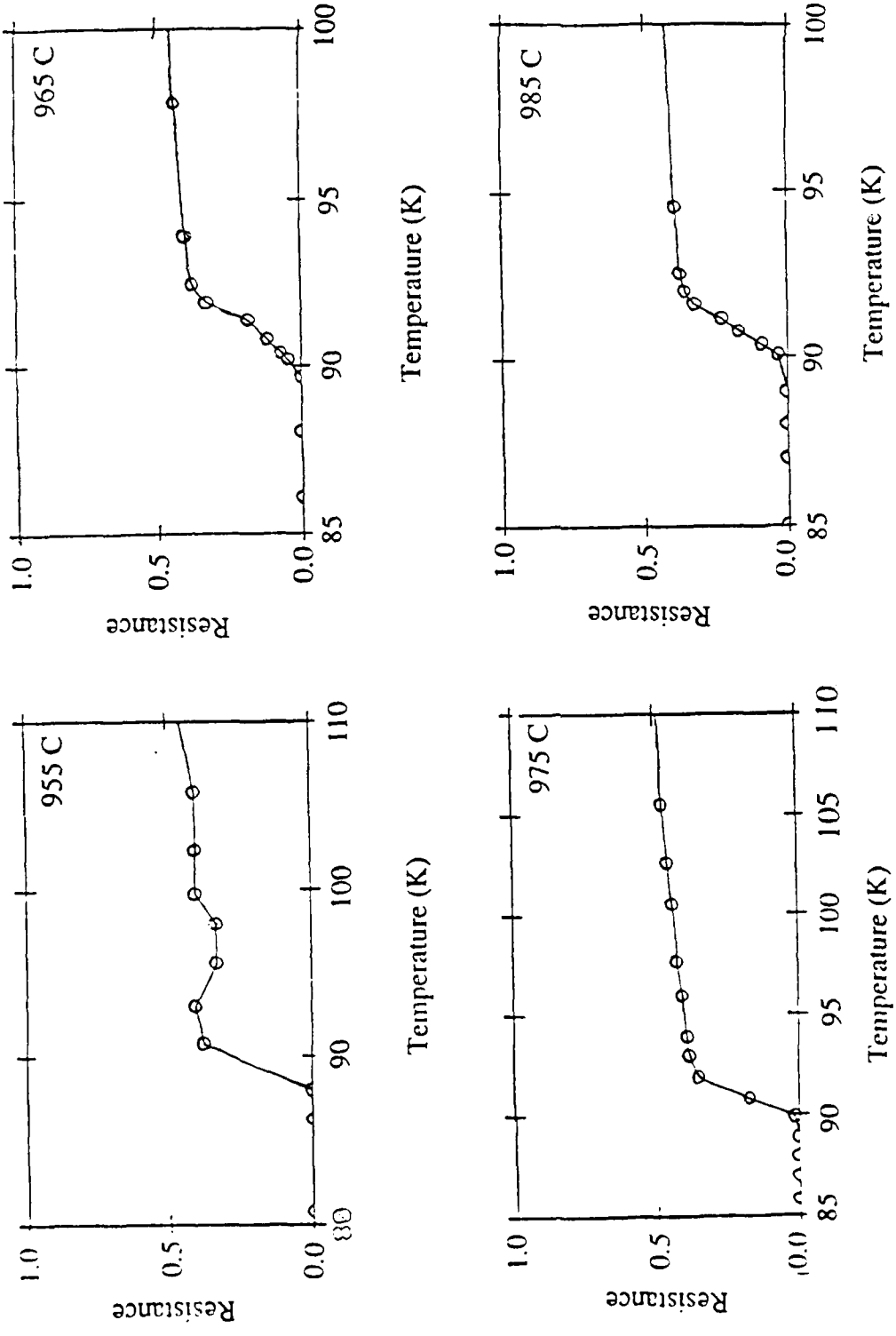

Figure 13. Four probe resistance for samples sintered at a) 955°C, b) 965°C, c) 975°C, and d) 985°C.

ELECTRONICS TECHNOLOGY AND DEVICES LABORATORY
MANDATORY DISTRIBUTION LIST
CONTRACT OR IN-HOUSE TECHNICAL REPORTS

Defense Technical Information Center*
ATTN: DTIC-FDAC
Cameron Station (Bldg 5)
Alexandria, VA 22304-6145

(*Note: Two copies for DTIC will be sent from STINFO Office.)

Director
US Army Material Systems Analysis Actv
ATTN: DRXSY-MP
001 Aberdeen Proving Ground, MD 21005

Commander, AMC
ATTN: AMCDE-SC
5001 Eisenhower Ave.
001 Alexandria, VA 22333-0001

Commander, LABCOM
ATTN: AMSLC-CG, CD, CS (In turn)
2800 Powder Mill Road
001 Adelphi, Md 20783-1145

Commander, LABCOM
ATTN: AMSLC-CT
2800 Powder Mill Road
001 Adelphi, MD 20783-1145

Commander,
US Army Laboratory Command
Fort Monmouth, NJ 07703-5000
1 - SLCET-DD
2 - SLCET-DT (M. Howard)
1 - SLCET-DB
35 - Originating Office

Commander, CECOM
R&D Technical Library
Fort Monmouth, NJ 07703-5000
1 - ASQNC-ELC-IS-L-R (Tech Library)
3 - ASQNC-ELC-IS-L-R (STINFO)

Advisory Group on Electron Devices
201 Varick Street, 9th Floor
002 New York, NY 10014-4877

Director
Naval Research Laboratory
ATTN: CODE 2627
001 Washington, DC 20375-5000

Cdr, PM JTFUSION
ATTN: JTF
1500 Planning Research Drive
001 McLean, VA 22102

Rome Air Development Center
ATTN: Documents Library (TILD)
001 Griffiss AFB, NY 13441

Deputy for Science & Technology
Office, Asst Sec Army (R&D)
001 Washington, DC 20310

HQDA (DAMA-ARZ-D/Dr. F.D. Verderame)
001 Washington, DC 20310

Dir, Electronic Warfare/Reconnaissance
Surveillance and Target Acquisition Ctr
ATTN: AMSEL-EW-D
001 Fort Monmouth, NJ 07703-5000

Dir, Reconnaissance Surveillance and
Target Acquisition Systems Directorate
ATTN: AMSEL-EW-DR
001 Fort Monmouth, NJ 07703-5000

Cdr, Marine Corps Liaison Office
ATTN: AMSEL-LN-MC
001 Fort Monmouth, NJ 07703-5000

Dir, US Army Signals Warfare Ctr
ATTN: AMSEL-SW-OS
Vint Hill Farms Station
001 Warrenton, VA 22186-5100

Dir, Night Vision & Electro-Optics Ctr
CECOM
ATTN: AMSEL-NV-D
001 Fort Belvoir, VA 22060-5677

Cdr, Atmospheric Sciences Lab
LABCOM
ATTN: SLCAS-SY-S
001 White Sands Missile Range, NM 88002

Cdr, Harry Diamond Laboratories
ATTN: SLCHD-CO, TD (In turn)
2800 Powder Mill Road
001 Adelphi, MD 20783-1145